# SCALING RELATION OF SEISMIC WAVE ENERGY IN TERMS OF MAGNITUDE, DISTANCE AND SITE CONDITION

**A DISSERTATION**

*Submitted in partial fulfillment of the requirements for the award of the degree*

*Of*

**MASTER OF TECHNOLOGY**

**In**

**EARTHQUAKE ENGINEERING**

(*With specialization in Structural Dynamics*)

*By*

**DHEERAJ VIRMANI**

**(15526004)**


**Department of Earthquake Engineering**

**Indian Institute of Technology, Roorkee**

**Roorkee – 247667, Uttarakhand, India**

May 2018

## CANDIDATE'S DECLARATION

I hereby declare that the work carried out in this seminar report entitled, "**SCALING RELATION OF SEISMIC WAVE ENERGY IN TERMS OF MAGNITUDE, DISTANCE AND SITE CONDITION",** is being submitted in partial fulfillment of the requirements for the award of degree of "Master of Technology" in Earthquake Engineering with specialization in Structural Dynamics submitted to the Department of Earthquake Engineering, Indian Institute of Technology Roorkee, under the supervision of **Dr. DAYA SHANKER**, Assistant Professor, and **Dr. I.D. GUPTA,** honorary fellow, Department of Earthquake Engineering, I.I.T. Roorkee.

I have not submitted the record embodied in this report, for the award of any other degree or diploma.

Place: Roorkee — Dheeraj Virmani

Date: — (15526004)

## CERTIFICATE

This is to certify that the above statement made by the candidate is correct to the best of my knowledge and belief.

**Dr. Daya Shanker**
Assistant Professor
Department of Earthquake Engineering
Indian Institute of Technology Roorkee

Place: Roorkee

Date:

# ACKNOWLEDGEMENT

I wish to express my deep sense of gratitude and indebtedness to my elite guide Dr. Daya shanker, Assistant Professor, Department of Earthquake Engineering, IIT Roorkee, for being helpful and great source of inspiration. I am thankful to him for his persistent interest, constant encouragement, vigilant supervision and critical evaluation. His encouraging attitude has always been a source of inspiration for me. His helping nature, invaluable suggestions and scholastic guidance are culminated in the form of the present work.

I am also thankful to Miss Neha Kumari, Mr. Naveen Kumar Kedia, Mr. Luv Joshi for their help, support and constant discussion throughout the report.

Place: Roorkee
Date:

Dheeraj Virmani
(15526004)

# ABSTRACT

As any earthquake occurs, a large amount of energy is released due to tectonic movement but as it is not the same when distributed in far distance areas, only a fraction of that part reaches to the considered location. So we are considering the energy which reaches the site and will cause damage to the structure. This seismic wave energy reaching considered site is advantageous over the earthquake intensities, arias intensity, PGA, PGV, PGD etc. because these factors are related to the energy at site which cannot be linked directly with the hazard. The wave energy reaching at site is calculated. Further for developing the relationship of this energy with magnitude, distance and site geology (soil depth) 42 earthquake data (229 earthquake records) are taken from PESMOS. After applying the base corrections to the data the random effect regression method is followed to develop the relations of energy with considered parameters.

# TABLE OF CONTENTS

# LIST OF FIGURE

# LIST OF TABLE

# CHAPTER 1

# INTRODUCTION

## 1.1 BACKGROUND

Earthquake is the disastrous phenomenon which causes catastrophic damage and great loss to living beings, since the beginning of history. Every moment, uncountable earthquakes occur on earth, some are measurable and some are not. These disasters are risk to human life and causes damage to their properties. The major motivation to study earthquakes is the damage caused by these earthquakes. With globalization, many have entered in the field of studying earthquakes, many researchers, seismologists and earthquake engineers are studying this field. Many a new theories and great achievements have been proposed.

If we need to understand earthquakes and structure of Earth, then we need a large number of observation stations, to monitor seismicity and record data of high quality. After collecting effective data inverse analysis and also statistical analysis can be carried out on data to understand the laws that control earthquake activities and to understand earth's structure. By identifying the earthquake prone regions and estimating, how likely earthquakes are going to occur and shaking they can produce, earthquake hazard can be reduced via resistant construction. However, without data, this is not possible. This data can be recorded by instruments installed on ground and these record ground motion as function of time, or seismograms. The data collected gives the better interpretation of earthquake. For studies, mostly three orthogonal components of seismograms are selected for analysis. In this thesis the three components of earthquake record are chosen to develop ground motion attenuation relationships.

The most important causes, due to which the damage occurs during earthquake is ground shaking. When the waves reach the earth surface they causes shaking which can last for seconds to minutes. These waves radiates from the source of earthquake and travel to far distances in different forms (S waves and P waves etc.). estimating ground shaking is the most important step in estimating the earthquake effect on people and structures. Earthquake can cause disaster and casualities in four ways. Firstly, damage caused to natural and artificial structures due to vibratory ground shaking. Secondly, rupture of fault, underground andat the

surface which causes damage to structure in nearby area. Third, in fault regionuplifting may cause damage and fourth, seiches and tsunamis may inundate coastal region which causes damage. So, to reduce the losses due to ground shaking much work has been done and ground motion attenuation relationships could be considered as one of these works. Ground motion attenuation relations are one of the most useful and significant research topic in engineering seismology. It is the basic for seismic design and seismic hazard analysis and seismic zonation map drawings etc. It is very closely related to human activities in common world.

The most important objective of seismology is to find critical indices of damage that are related to parameters of ground motion. Quantification of the ground motion needs a good understanding of the ground motion parameters which characterize the severity and damage potential of earthquake and seismological, topographical and geological factors which affect them. It is required to minimize the variability in correlation between the damage index and the selected ground motion parameters so as to obtain accurate prediction as possible of level of anticipated damage. The response spectrum superposition is practical tool for design of the structures expected to vibrate without any damage during largest possible level of shaking. But pragmatic consideration, analysis of the uncertainties and minimization of cost results in design of structure which may experience damage from the rare and strong earthquake shaking. So, during last some years many modifications have been introduced in the response spectrum method so as to reconcile its linear nature along with its desired non linear use in the design. This thesis explores the alternative to spectral method in the earthquake resistant design, by analyzing flow of energy associated with the strong motion. It requires consideration of all principal stages of the earthquake energy flow, from earthquake source, along propagation path and to final work leading to the relative response of structure. Loss of the energy along propagation path has to be considered. All these losses has to be accounted for to accurately quantify remaining energy which will excite relative response of structures.

A Well-designed structure is expected to be ductile during the largest shaking and to have a very large energy reserve so as to at least delay failure, if it cannot be avoided. As the structure finally enters to large nonlinear level of response, it absorbs excess of input energy through the ductile deformation of its components. So, it is logical to form the earthquake resistant design procedures in the terms of energy driving the process. The major advantage of using energy is that, duration of strong motion, number of cycles to failure, dynamic instability, all of these can be considered directly and explicitly. This requires the scaling of earthquake sources and attenuation of strong motion to be described as energy terms. Idea to

use energy parameters in seismic design is traced back to 1930's, when benioff proposed use of seismic destructiveness to be measured by calculating area under relative displacement response spectrum. Seismological and earthquake engineering characterization of earthquake source begins with estimation of its size. For centuries, it was done in terms of the earthquake intensity scales and these are not instrumental and these are based on human description of effect of earthquake.

## 1.2 OBJECTIVEOF THE STUDY

The objective is to establish relation, for a particular site, for the wave energy transmitted through the site and energy transmitted to the structure in that area. The relation between the magnitude of earthquake in that region and energy which is being transmitted to the site and to structure at site will be established. This energy transmission depends on the site condition of the area and the distance of the structure from the epicenter. We will collect the earthquake data for a particular site (such as isoseismal maps, magnitude, intensity etc.) and based on collected data best suited relationship will be formed.

For calculating this energy relations site-specific design response spectra and attenuation relationship are required to represent the dependence on earthquake magnitude, source-to-site distance , duration of ground shaking and local soil and site geological conditions

# CHAPTER 2

## LITERATURE REVIEW

**Hirai.T and Sawada.S(2008)** The characteristics of seismic wave energy are examined in this study. The attenuation equation of total seismic wave energy with respect to moment magnitude and hypocentral distance is proposed in order to estimate the seismic intensity. It is concluded that the total seismic wave energy should be better than PGA to estimate seismic motion with respect to earthquake magnitude stably. In this engineering base layer is chosen whose S-wave velocity are greater than 300 m/s. the attenuation equation used for regression analysis used is

$$\log (E) = a M_w - b*\log (X) + c$$

where E is seismic wave energy in joule/ meter square, $M_w$ is moment magnitude, x is hypocentral distance in kms and a,b,c are regression coefficient. Further wavelet transformation is used for time- frequency analysis. Further it is concluded that in low frequency range the effect of earthquake magnitude is more on seismic wave energy. As hypo central distance is increased, in hgh frequency range, seismic wave energy decreases rapidly. It shows that in high frequency range the internal damping factor is large.

**Danciu.L and Tselentis.G.A(2007)** Describes the steps involved in developing new attenuation relationships for different parameters using all existing and up to date Greek strong motion data. Input energy is described as better to use in design purpose as it has potential to address effects of duration and hysteretic behavior. The strong motion data to develop attenuation relationship of engineering ground motion, is taken from European strong motion database. The dataset consists of 335 records from 151 Greek earthquake. Magnitude range is between 4.5 to 6.9. The non-linear mixed effect model is used to develop attenuation relationships. The relationship between explanatory variable (magnitude) and response variable ( PGA ) is non-linear. The values of coefficient and empirical equation is developed using two step regression. The developed attenuation relationships could provide

an improvement criteria for the selection of earthquake scenarios in terms of engineering ground motion parameters that are most representative of structural damage.

**Trifunac.M.D (2007)** This note is the first in a series devoted to a study of the flow of earthquake energy from the source to its destination, the soil–structure systems, where it will drive the relative structural response. The basic seismological aspects of empirical scaling of seismic wave energy, Es, are reviewed, and it is shown how this energy can be represented by functionals of strong ground motion. This constitutes the first required step, after which this energy will be attenuated (dissipated) along the wave propagation path, arriving as the incident-wave energy upon the soil–structure systems. The ultimate goal of this work is to form a basis for formulation of a new design method in which the power of the incident-wave pulses will be compared with the capacity of the structure to absorb this power. This paper explores an alternative to the spectral method in earthquake-resistant design, by analyzing the flow of energy associated with strong motion. This requires consideration of all of the principal stages of earthquake energy flow, from the earthquake source, along the propagation path, and to the final work leading to relative response of the structure. The loss of energy along the propagation path also has to be considered. These losses must be accounted for to properly quantify the remaining energy, which will excite the relative response of the structures. In this, the first in a series, we will analyze only the strong-motion estimates of earthquake energy release at the source.

**Ozbey.C,et.al. (2003)**An important component of seismic hazard analysis is to provide a proper model used for predicting the expected ground motion distribution for a possible earthquake scenario, which should consider the characters of earthquake sources, the paths of wave propagation and local site conditions. In this thesis, 249 earthquake recordings were selected with 3 orthogonal-component seismograms both from Chinese (including Taiwan) and Japanese database. The widely used ground motion attenuation model is adopted to construct the empirical attenuation equations by two-step regression method proposed by Joyner and Boore [1981]. The predicted peak ground parameters are expressed as a function of magnitude, distance (epicentral distance or hypocentral distance) and site category. The model uses a magnitude-independent shape according to geometrical spreading and anelastic attenuation for the attenuation relationships. The final results then are compared with previous attenuation equations obtained by other authors.

**Boore.D.M and Boomer J.J (2004)** Recordings from strong-motion accelerographs are of fundamental importance in earthquake engineering, forming the basis for all characterizations of ground shaking employed for seismic design. The recordings, particularly those from analog instruments, invariably contain noise that can mask and distort the ground-motion signal at both high and low frequencies. For any application of recorded accelerograms in engineering seismology or earthquake engineering, it is important to identify the presence of this noise in the digitized timehistory and its influence on the parameters that are to be derived from the records. If the parameters of interest are affected by noise then appropriate processing needs to be applied to the records, although it must be accepted from the outset that it is generally not possible to recover the actual ground motion over a wide range of frequencies. There are many schemes available for processing strong-motion data and it is important to be aware of the merits and pitfalls associated with each option. Equally important is to appreciate the effects of the procedures on the records in order to avoid errors in the interpretation and use of the results. Options for processing strong-motion accelerograms are presented, discussed and evaluated from the perspective of engineering application.

**Khashaee.p,et.al.(2003)** In developing an energy-based design approach and assessing the damage potential of structures, one must know the distribution of earthquake input energy among energy components: kinetic, elastic strain, hysteretic, and damping. This report examines the influences of the ground motion characteristics: intensity, frequency content, and duration of strong motion and the structural properties: ductility, damping, and hysteretic behavior on the distribution of input energy for a one- and a five-story building using 20 accelerograms, ten with short and ten with long duration of strong motion. Results indicate that for certain damping ratios, ductility has a significant influence on input energy and its distribution among energy components in a structure. For a given ductility ratio, small damping ratio (less than 5%) has a minor effect on input energy, but a major influence on the energy distribution. Damping ratios larger than 5% have a significant influence on the input energy and its distribution. Three energy ratios that relate to hysteretic energy were computed: the maximum ratio of hysteretic to input energy $(E_h/E_{ir})_m$, the ratio of the maximum hysteretic energy to the maximum input energy $E_{hm}/E_{irm}$, and the equivalent number of yield excursions $N_{eq}=E_{hm}/(F_y.u_p)$ where $F_y$ is the yield strength, and $u_p$ is the plastic deformation. It is found that $(E_h/E_{ir})_m$ generally reflects the energy demand for the largest

yield excursion, and $E_{hm}/E_{irm}$ and $N_{eq}$ reflect the energy demand for the entire duration of accelerogram. The study shows that $(E_h/E_{ir})_m$ is independent of the duration of strong motion and period of structure; however, $E_{hm}/E_{irm}$ is independent of both only for periods less than 1 s. Results indicate that as the duration becomes longer the equivalent number of yield excursions $N_{eq}$ increases indicating more structural damage.

# CHAPTER 3

# SEISMIC WAVE ENERGY AND OTHER PARAMETERS

## 3.1 INTRODUCTION

The current seismic design practices are based on strength principle i.e. using acceleration spectra. By multiplying the mass of building with the acceleration at natural period of structure will result in the lateral force applied on structure. But the peak ground acceleration is not the best indicator of structural damage because large recorded PGA associated with short duration usually causes less damage but moderate PGA with long duration causes much more damage. In first case, the seismic energy is absorbed by inertia of structure with less deformation. But in second case, more moderate acceleration results in significant damage of structure. The strength principles do not account for duration of strong motion or hysteretic behavior of structure but design approach based on input energy has potential to address directly the effects of duration as well as hysteretic behavior.

The earthquake vibrations originate from point of initiation of the rupture and propagate in every direction. These vibrations travel in the form of elastic waves through the rocks. Mainly three types of waves are associated with the propagation of elastic stress wave generated by the earthquake. These waves are primary waves (P), secondary waves (S) and surface waves.

These waves produced at source of earthquake, contain a large amount of energy, which can be expressed in terms of magnitude. But they carry only fraction of energy after reaching the considered location.

## 3.2 EARTHQUAKE INPUT ENERGY

The earthquake input energy, which is transmitted to a structure, consists of the elastic strain energy, kinetic energy, damping energy, and hysteretic energy. The kinetic energy reflects the work done by the inertia force. Elastic strain energy is the input energy stored in structure in the form of elastic strain. The damping energy is work of damping force. The

hysteretic energy is the energy that is dissipated through hysteretic action and it is associated with the damage potential of structure (Kuwamura and Galambos, 1989).

## 3.3 DEFINITION OF SEISMIC WAVE ENERGY

There are several studies for the seismic wave energy. We adopt the definition of total seismic wave energy passing through the unit volume as

Two procedures for computing the earthquake input energy are proposed by Uang and Bertero (1990)

1) Based on the absolute motion

2) Relative motion.

Difference between these two procedures is not that important in damage assessment because the hysteretic energy, which is associated with damage potential of the structures, does not depend on the approach used. However, elastic input energy using relative motion is considered more useful than input energy in terms of the absolute motion as all internal forces within the structures are computed using relative displacement and velocity. So , the procedure based on the relative displacement is preferred.

## 3.4 EARTHQUAKE WAVE ENERGY FLOW AND DISTRIBUTION:

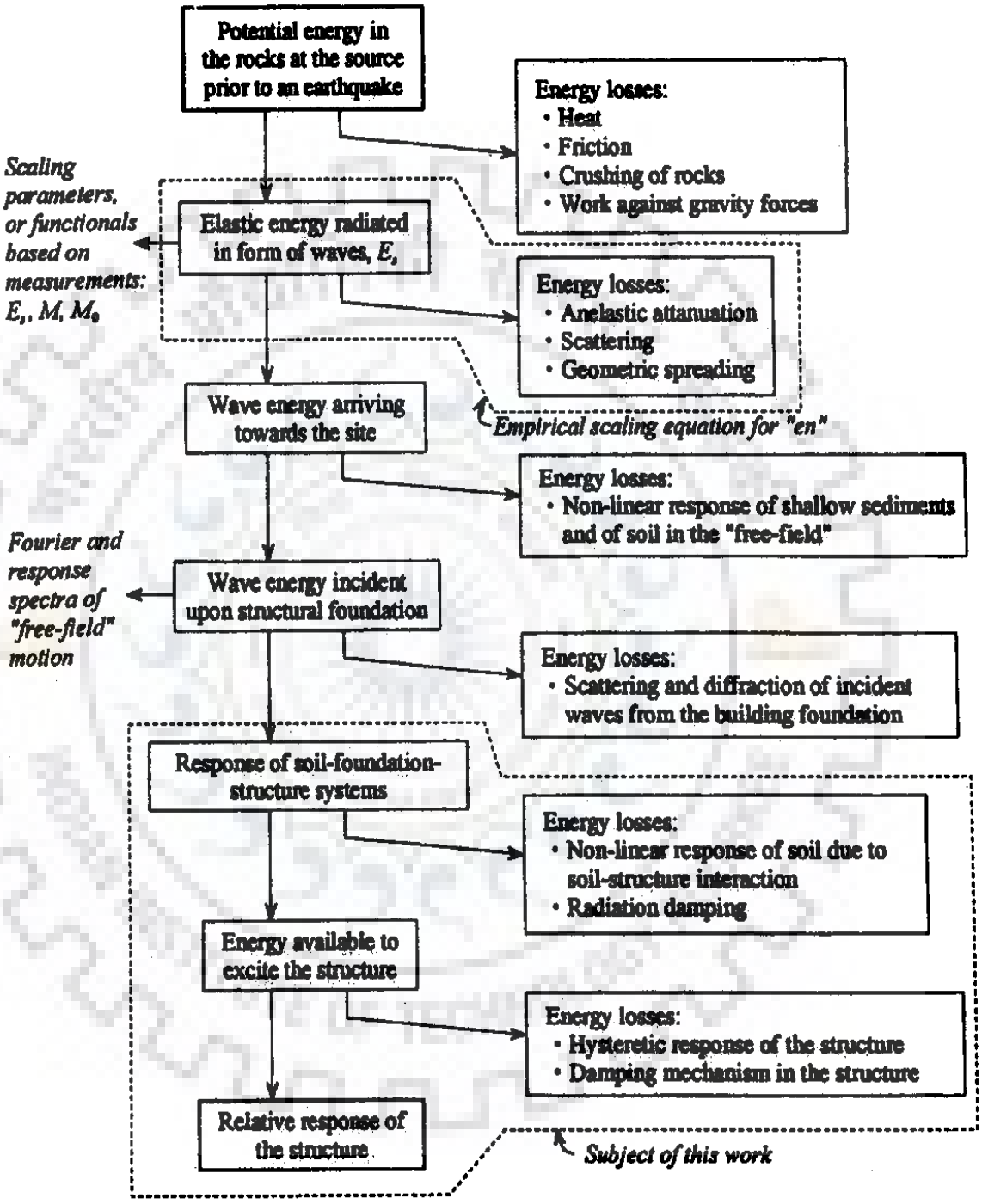


Fig 3.1 - Earthquake wave energy flow diagram

## 3.5 ENERGY BALANCE EQUATION

The energy balance equation for an SDOF structure can be written as [6]

$$\int_0^t m\,\ddot{u}\,\dot{u}\,dt + \int_0^t c\,\dot{u}^2\,dt + \int_0^t f\,\dot{u}\,dt = -\int_0^t m\,\ddot{u}\,\dot{u}\,dt \qquad (3.1)$$

Where m is mass of the structure, c is the damping coefficient, *f* is the restoring force, u is the relative displacement of the mass with respect to ground, $\dot{u}$ is the velocity of the mass with respect to ground, $\ddot{u}$ is the acceleration of the mass with respect to ground, and t is time. The energy balance equation (3.1) can be written as

$$E_{kr} + E_d + E_a = E_{ir} \qquad (3.2)$$

Where $E_{kr}$ is the relative kinetic energy, $E_d$ is the damping energy, Ea is the absorbed energy, and $E_{ir}$ denotes the relative input energy such that

$$E_{kr} = \frac{1}{2} m\,\dot{u}^2 \qquad (3.3)$$

$$E_d = \int_0^t c\,\dot{u}^2\,dt \qquad (3.4)$$

$$E_a = \int_0^t f\,\dot{u}\,dt \qquad (3.5)$$

$$E_{ir} = -\int_0^t m\,\ddot{u}\,\dot{u}\,dt \qquad (3.6)$$

The absorbed energy consists of the recoverable elastic strain energy $E_s$ and the irrecoverable hysteretic energy $E_h$ where

$$E_s = \frac{f^2}{2K} \qquad (3.7)$$

$$E_h = E_a - E_s \qquad (3.8)$$

Here k is the pre-yield stiffness of the structure.

## 3.6 EXISTING PROCEDURES FOR COMPUTING INPUT ENERGY

1. Housner (1956) computed the input energy per unit mass as

$$\frac{E}{m} = \frac{1}{2}(PSV)^2 \qquad (3.9)$$

Where m gives the mass and PSV is the pseudo-spectral velocity. He used this equation for elastic and inelastic behavior.

2. Zahrah and Hall (1984) computed the input energy per unit mass as

$$\frac{E}{m} = -\int_0^t \ddot{U}\dot{U}\, dt \qquad (3.10)$$

3. Akiyama (1985) proposed the input energy per unit mass for an elastic SDOF structure as

$$\frac{E}{m} = \frac{1}{2}(V)^2 \qquad (3.11)$$

Where V is an equivalent velocity.

$V = 2.5\ T_N$ $\qquad T_N < T_G$

$V = 2.5\ T_G$ $\qquad T_G < T_N$

where $T_G$ is the predominant period of ground motion as a function of soil type. The values of T are 0.4, 0.6, 0.8, and 1.0 s for soil types I (bed rock), II, III, and IV (softest soil), respectively

One more recommendation is

$$\frac{E}{m} = 2.2\ (t)^{.5}(PGV)^2 \qquad (3.12)$$

In which‘t’ is the duration of strong motion defined by Trifunac and Brady (1975), and PGV is the peak ground velocity.

## 3.7 WAVE ATTENUATION

The seismic energy cannot be transmitted perfectly by Earth. As the distance from focus increases, the energy attenuates. As it is known, earth is an inelastic material, so anelastic losses occur, that attenuate the wave energy progressively. The anelasticity changes the pulse shape, causes depression and affect the amplitude of waves.

Mainly there are two types of attenuation effects, either intrinsic anelasticity, that is associated with small scale crystal dislocation, movement of interstitial fluids and friction or scattering attenuation anelastic process of redistributing wave energy by refraction, reflection and conversion at irregularities in the medium. Also, geometric spreading of wave energy is cause of ground motion attenuation. With increase in distance from focus, the seismic energy on unit area decreases. The earth medium is very complex material. There are so many issues associated with the wave energy attenuation. But, simple models are used to simulate ground motion attenuation based on main attenuation mechanism.

Amplitudes of seismic waves are not only controlled by geometrical spreading or focusing and by the reflection and transmission coefficients that occur at discontinuities. Besides this, wave amplitudes may be reduced because of energy loss due to inelastic material behavior or internal friction during wave propagation. These effects are called intrinsic attenuation. Also, scattering of energy at small-scale heterogeneities along the travel paths may reduce amplitudes of seismic waves. In the case of such scattering attenuation, however, the integrated energy in the total wave field remains constant, while intrinsic attenuation results in loss of mechanical wave energy, e.g., by transformation into heat. The wave attenuation is usually expressed in terms of the dimensionless quality factor Q

$$Q = 2\rho E/DE \qquad (3.13)$$

With DE the dissipated energy per cycle. Large energy loss means low Q and vice versa, i.e., Q is inversely proportional to the attenuation.

## 3.8 METHODS TO MEASURE EARTHQUAKES

### 3.8.1 INTENSITY

The intensity of an earthquake refers to the degree of destruction caused by it. In other words, intensity of an earthquake is a measure of severity of the shaking of ground and its attendant damage. This, of course, is empirical to some extent because the extent of destruction or damage that takes place to a construction at a given place depends on many factors. Some of these factors are:

1) distance from the epicenter,
2) compactness of the underlying ground,
3) type of construction
4) magnitude of the earthquake
5) duration of the earthquake and
6) depth of the focus. Intensity is the oldest measure of earthquake

Numerous intensity scales have been developed over the last several hundred years to evaluate the effects of earthquakes, the most popular is the Modified Mercalli Intensity (MMI) Scale

Relationships correlating earthquake intensity to peak ground velocity is given by

$$\text{MMI} = \frac{\log 14V}{\log 2} \qquad (3.14)$$

Where Vis the peak ground velocity in cm/sec.

Another such relation reported by Wald et.al, (1999) based on Californian earthquake database is

$$\text{MMI} = 3.47 \log(\text{Vg}) + 2.35\ (1.5) \qquad (3.15)$$

In addition to peak ground velocity, empirical relationships correlating peak ground acceleration to MMI has also been reported. For e.g.,

$$\text{MMI} = 3.66 \log (\text{Peak Ground Acceleration in cm/sec/sec}) - 1.66 \qquad (3.16)$$

Arias intensity (*Ia*), as defined by Arias (1970), is thetotal energy per unit weight stored by a set of undampedsimple oscillators at the end of the ground motion. The Arias intensity for ground motion in the *x* direction ($I_{ax}$), is calculated as follows:

$$I_{ax} = \frac{2\pi}{g}\int_0^t [\, a(t)\,]^2\, dt \qquad (3.17)$$

Where a(t) is the acceleration time history in the x direction, and t is the total duration of ground motion. $I_{ax}$is a measure of energy, which is scalar in nature, and Ia in the presentinvestigation is considered as the sum of the two horizontal components (east–west and north–south), calculated as follows:

$$I_a = I_{ax} + I_{ay} \qquad (3.18)$$

### 3.8.2 MAGNITUDE

The magnitude of an earthquake is related to the amount of energy released by the geological rupture causing it, and is therefore a measure of the absolute size of the earthquake, without reference to distance from the epicenter.

Some relationships between energy and magnitude given by guttenberg are:

$$\text{Log } E = 9.4 + 2.14M - 0.054M \qquad (3.19)$$

A numerical equivalent, for M from 1 to 8.6, is

$$\text{Log } E = 9.1 + 1.75M + \log (9 - M) \qquad (3.20)$$

If $M_s$ results from surface waves, $M_B$ from body waves, approximately

$$M_s - M_B = 0.4\,(M_s - 7) \qquad (3.21)$$

These are the energy produced at the source of earthquake.

# CHAPTER 4

# SITE CHARACTERIZATION AND DATABASE

## 4.1 INTRODUCTION

The Himalayan frontal arc constitutes the central part of the Alpide seismic belt. As far as earthquakes are concerned, this is one of the most active intra-continental regions in the world. The northward movement of the Indian plate caused continental collision and created the Himalayan mountain range. The current seismic activity is the result of the continental collision between the Indian and the Eurasian plates. The instrumental recording in the region started towards the end of the 19th Century with the installation of Milne seismograph at Alipore, Calcutta in 1998 and later at Colaba, Bombay and Madras.

## 4.2 TECTONICS SETUP OF AREA AND TECTONIC MAP

The tectonic features refer to the geological structures like faults, folds, rifts and shear zones which may be the probable sources of earthquakes in a region. These features are shaped by the interaction of the Indian plate with the Eurasian plate under the framework of plate tectonics (Molnar, 1988). With the continued movement of the Indian plate in NE direction, large scale folding, crustal shortening and vertical crustal movements have taken place, forming the great Himalayas and other subsidiary faults in the region.

The area can be divided longitudinally into five major crustal formation zones (Gupta, 2006). These can be identified from south to north as follows:

(i) Outer zone of the fore-deep.

(ii) Inner zone of the fore-deep forming the Himalayan foot-hills.

(iii) Lesser Himalaya formed by superposition of a series of tectonic nappesthrusted over the fore-deep.

(iv) High Himalaya

(v) Indus-Tsangpo Suture zone.

The first four of these zones are separated from each other by large thrust faults. The Main Frontal Thrust (MFT) runs at the boundary between the outer and the inner zones of the

fore-deep. The Main Boundary Thrust (MBT) separates the napped-folded complex of the Lesser Himalaya (mainly composed of deposits of Proterozoic and Precambrian age) from The Himalayan foot-hills made up essentially of Tertiary and Quaternary sediments. The MBT is tectonically the most active feature at present time. Neotectonic activity has been also recorded at several places along the FHT running in the Siwalik deposits in front of the MBT. The belt north of High Himalaya and bound by Indus-Tsangpo Suture is known as Tethys Himalaya, which consists of fossil ferrous sedimentary rocks. The trans-Himalayan zone includes the Kailas and Laddakh ranges and continues up to the Tibetan plateau. This includes the Indus Suture Zone. The belt between the Karakoram Fault and ISZ is occupied by cover rocks affected by the Himalayan orogeny. Neotectonic activity has been recorded along the Karakoram Fault and the ISZ. In the central part of the region of Fig. 3.2, several subsidiary thrusts exist between MBT and MFT, some of which are tectonically active and have considerable spatial extent. The Jwalamukhi and Drang Thrusts are the two most significant subsidiary thrusts. The Himalayan thrust faults are divided into segregate fragments up to 100-150 km in length by a large number of strike-slip transverse faults all along their length. Where these longitudinal faults cross the Himalayan thrust belt, the earthquake activity is associated with both the thrust and the strike-slip faulting. The Sundernagar Fault, about 50 km east of project sites, is an important dextral transverse structure, which extends from High Himalayas to the Frontal Belt. This fault is considered to have caused the swing of the Frontal Belt from NW-SE to N-S. The Kaurik Fault system in the high Himalayas is another significant transverse feature, rupturing along which is considered to have generated the M6.2 Kinnaur earthquake of 19 January 1975. There are several other lineaments transverse to the Himalayan trend, whereas a few are sub-parallel to it. As the transverse features segregate the Himalayan longitudinal trend into several independent segments, the region of Fig. 3.2is considered adequate to represent the seismic potential of all the tectonic features of significance to the project sites.

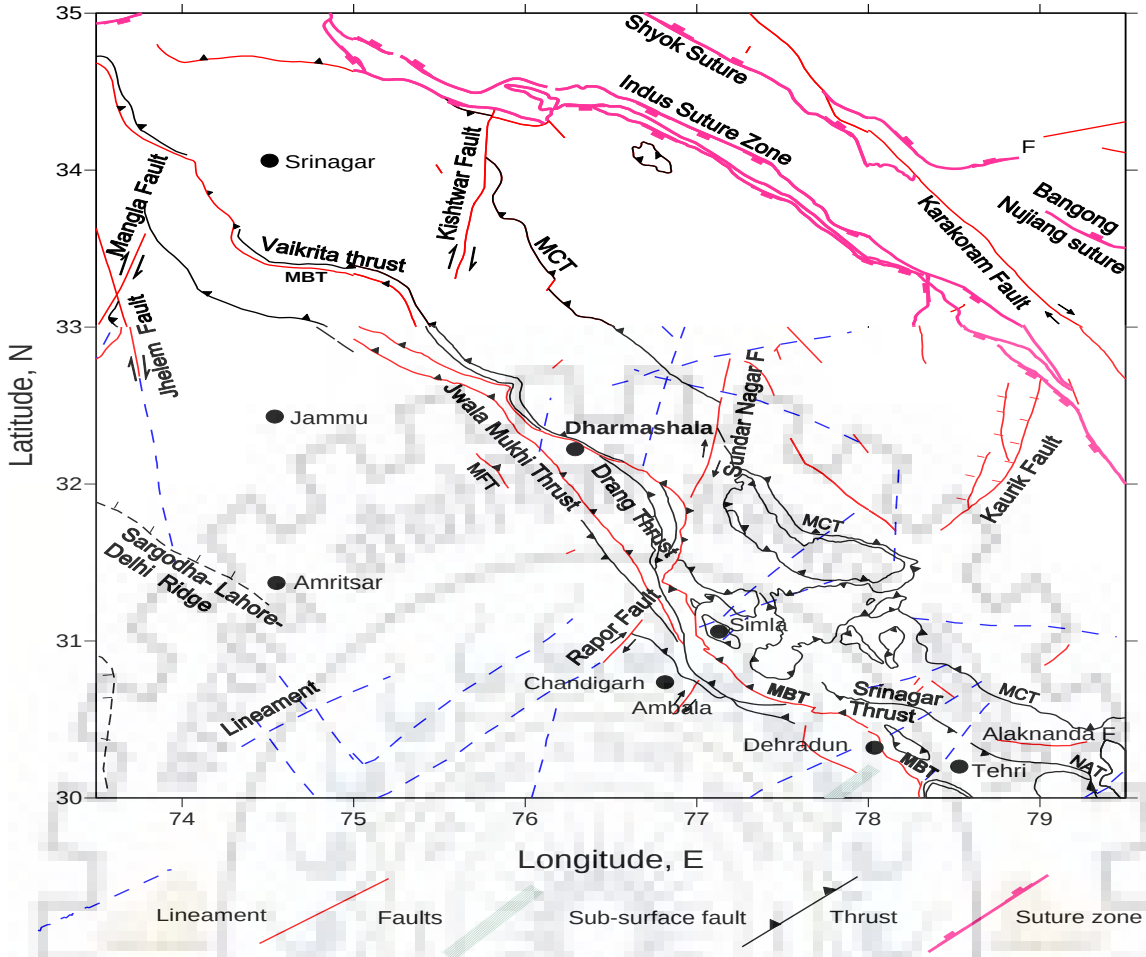


**Figure 4.1** -Tectonic map of area

## 4.3 DATA BASE

In the present study, the instrumental data have been collected from the website of Pesmos of www.pesmos.in [15] of IIT Roorkee. There is Installation of 300 strong motion accelerographs in seismic zones IV and V and some thickly populated cities of zone III in North and North East part of country and 298 instruments have been installed in the states of Uttarakhand, HP, Punjab, Delhi, Rajasthan, Haryana, Bihar, WB, Sikkim, A&N, UP, Assam, Meghalaya and Mizoram from where data is collected.[7]

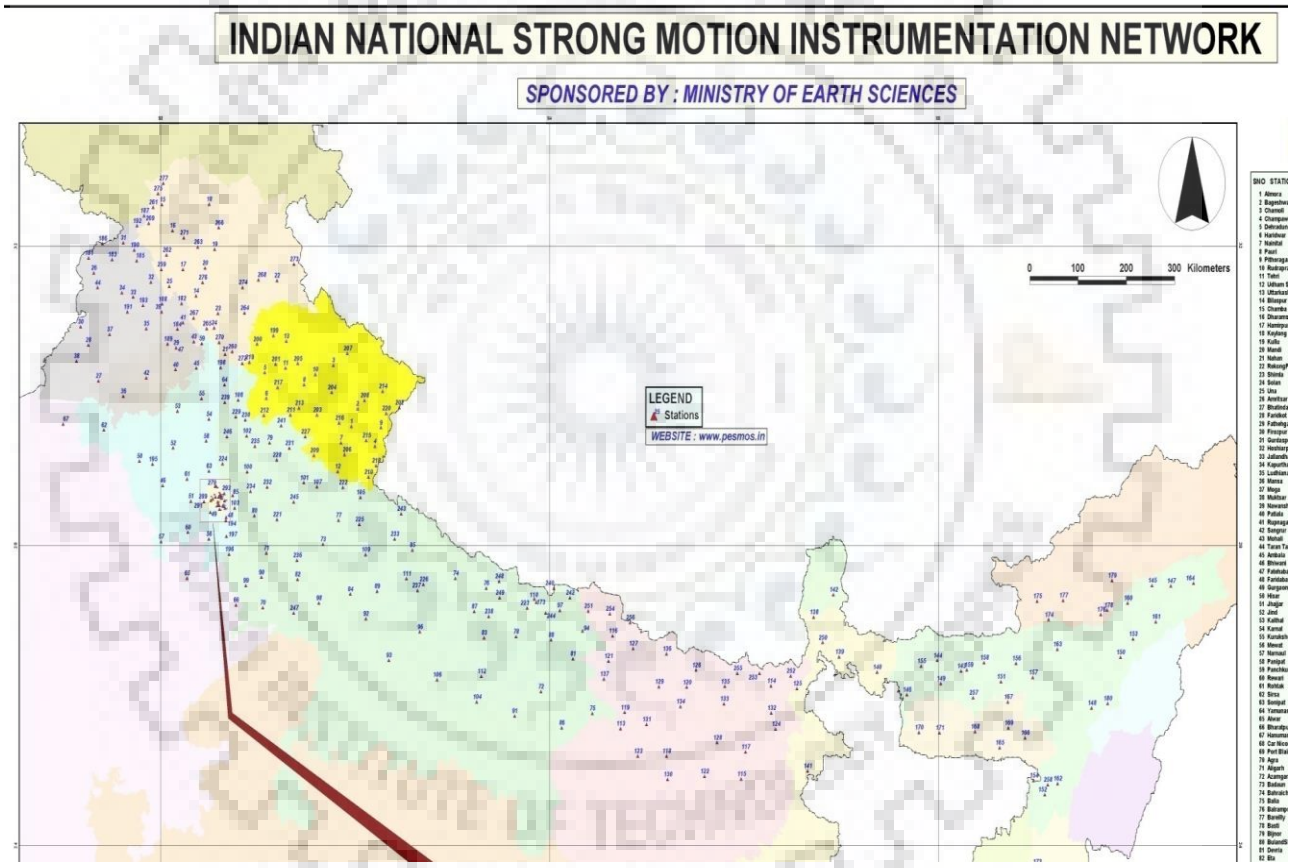


**Fig 4.2** - ACCELEROGRAPHS PICTURE

The Himalayan range earthquake strong-motion records are used for the study of the attenuation relationships of engineering ground motion [1]. The final dataset consists of 687 records from 229 earthquakes. The magnitude scale corresponds to the moment magnitude (Hanks and Kanamori, 1979). For the selected dataset based on data, M ranges between 3.3 and 6.4. Hypocentral depths of the selected earthquakes are in the interval 0 to 79 km with a mean of 21.14 kms. The table consisting of all the earthquake data that has been used to study and for calculations is as below.

**Table 4.1 -** List of strong ground motion record used for development of Attenuation Relationship

| No. | Earthquake Name | Date | Time | Latitude | Longitude | Focal depth | Magnitude | Number of Records |
|---|---|---|---|---|---|---|---|---|
| 1 | Kangra, Himachal | 26.04.1986 | 13:05:16 | 32.175 | 76.287 | 7 | 5.5 | 9 |
| 2 | Uttarkashi Earthquake | 20.10.1991 | 2:53:14 | 30.77 | 78.791 | 13.2 | 6.8 | 13 |
| 3 | Chamba Earthquake | 24.03.1995 | 17:22:32 | 32.668 | 76.167 | 29.2 | 4.4 | 2 |
| 4 | Chamoli Earthquake | 29.03.1999 | 0:35:12 | 30.41 | 79.42 | 21 | 6.5 | 10 |
| 5 | Chamoli,Uttarakhand | 14.12.2005 | 7:09:48 | 30.515 | 79.25 | 36.9 | 5.1 | 8 |
| 6 | Uttarkashi,Uttarakhand | 22.07.2007 | 23:02:12 | 31.2 | 78.2 | 33 | 4.9 | 2 |
| 7 | Pithoragarh,Uttarakhand | 19.08.2008 | 10:54:26 | 30.035 | 80.07 | 19.1 | 4.3 | 3 |
| 8 | Uttarakhand-Tibet | 04.09.2008 | 12:53:21 | 30.242 | 80.382 | 8.9 | 4.6 | 7 |
| 9 | Kullu,Himachal | 21.10.2008 | 15:09:06 | 31.5 | 77.3 | 10 | 4.3 | 3 |
| 10 | Kinnaur,Himachal | 09.01.2009 | 12:40:18 | 31.801 | 78.331 | 12 | 4.3 | 2 |
| 11 | Chamba,Himachal | 31.01.2009 | 3:07:15 | 32.507 | 76.492 | 11.5 | 3.8 | 3 |
| 12 | Bageshwar,Uttarakhand | 01.05.2009 | 22:36:25 | 29.9 | 80.1 | 10 | 4.6 | 7 |
| 13 | Chamba,Himachal | 17.07.2009 | 11:07:47 | 32.509 | 76.719 | 42 | 4.6 | 3 |
| 14 | Pithoragarh,Uttarakhand | 27.08.2009 | 16:54:15 | 30 | 80 | 14 | 3.8 | 3 |
| 15 | Uttarkashi,Uttarakhand | 21.09.2009 | 9:43:47 | 30.831 | 79.027 | 52.5 | 4.7 | 11 |
| 16 | Bageshwar,Uttarakhand | 03.10.2009 | 5:20:54 | 30.018 | 79.827 | 24.5 | 4.4 | 3 |

| | | | | | | | | |
|---|---|---|---|---|---|---|---|---|
| 17 | Tisa,Himachal | 11.01.2010 | 5:15:13 | 29.766 | 80.5 | 13.7 | 4 | 4 |
| 18 | Bageshwar,Uttarakhand | 22.02.2010 | 17:23:43 | 29.987 | 80.069 | 20.5 | 4.3 | 5 |
| 19 | Tibet | 26.02.2010 | 4:42:33 | 28.507 | 86.776 | 79 | 4.9 | 6 |
| 20 | Himachal | 14.03.2010 | 6:53:21 | 31.608 | 76.044 | 35 | 4.5 | 11 |
| 21 | Uttarakhand | 03.05.2010 | 17:15:08 | 30.4 | 78.4 | 8 | 3.8 | 4 |
| 22 | Himachal | 28.05.2010 | 7:25:06 | 31.2 | 77.9 | 43.8 | 4.6 | 4 |
| 23 | Almora,Uttarakhand | 31.05.2010 | 11:37:04 | 29.955 | 79.976 | 10 | 3.6 | 2 |
| 24 | Uttarakhand-Nepal | 06.07.2010 | 19:08:20 | 29.805 | 80.41 | 14.2 | 4.6 | 2 |
| 25 | Almora,Uttarakhand | 10.07.2010 | 3:16:20 | 30.009 | 79.614 | 6.6 | 4.2 | 4 |
| 26 | Uttarkashi,Uttarakhand | 09.02.2011 | 19:17:29 | 30.9 | 78.2 | 10 | 5 | 4 |
| 27 | Uttarakhand-Nepal | 04.04.2011 | 11:31:40 | 29.626 | 80.729 | 17.4 | 5.6 | 23 |
| 28 | Pithoragarh,Uttarakhand | 15.06.2011 | 0:59:28 | 30.6 | 80.1 | 10 | 3.3 | 2 |
| 29 | Chamoli,Uttarakhand | 20.06.2011 | 6:27:18 | 30.551 | 79.319 | 26.6 | 4.9 | 12 |
| 30 | Western Nepal | 26.02.2012 | 23:08:42 | 29.6 | 80.8 | 10 | 4.1 | 2 |
| 31 | Western Nepal | 23.08.2012 | 16:30:19 | 28.47 | 82.69 | 28.4 | 4.6 | 3 |
| 32 | Western Nepal | 11.11.2012 | 18:39:19 | 29.46 | 81.479 | 37.1 | 4.9 | 3 |
| 33 | Uttarkashi,Uttarakhand | 27.11.2012 | 12:15:15 | 30.9 | 78.422 | 23.4 | 4.8 | 4 |
| 34 | Western Nepal | 02.01.2013 | 17:42:15 | 29.4 | 81.1 | 10 | 4.5 | 2 |
| 35 | Western Nepal | 09.01.2013 | 7:44:20 | 29.694 | 81.711 | 34.2 | 4.3 | 4 |
| 36 | Uttarkashi,Uttarakhand | 11.02.2013 | 10:48:55 | 31 | 78.4 | 5 | 4.2 | 3 |
| 37 | J&K-Himachal | 01.05.2013 | 6:57:12 | 33.061 | 75.863 | 9.8 | 5.6 | 21 |
| 38 | J&K-Himachal | 02.08.2013 | 2:32:05 | 33.232 | 75.906 | 18.4 | 5.3 | 3 |
| 39 | Himachal-Punjab | 29.08.2013 | 10:13:21 | 31.55 | 76.301 | 31 | 4 | 8 |

| | | | | | | | | |
|---|---|---|---|---|---|---|---|---|
| 40 | Chamba-Himachal | 17.06.2014 | 17:31:08 | 32.2 | 76.1 | 10 | 3.9 | 2 |
| 41 | Chamba-Himachal | 21.08.2014 | 8:11:17 | 32.283 | 76.347 | 10 | 4 | 2 |

The magnitude range and focal depth range is plotted with respect to the number of earthquakes and number of records as per figure number 2.4 and 2.5 respectively to describe clearly the record used for the study

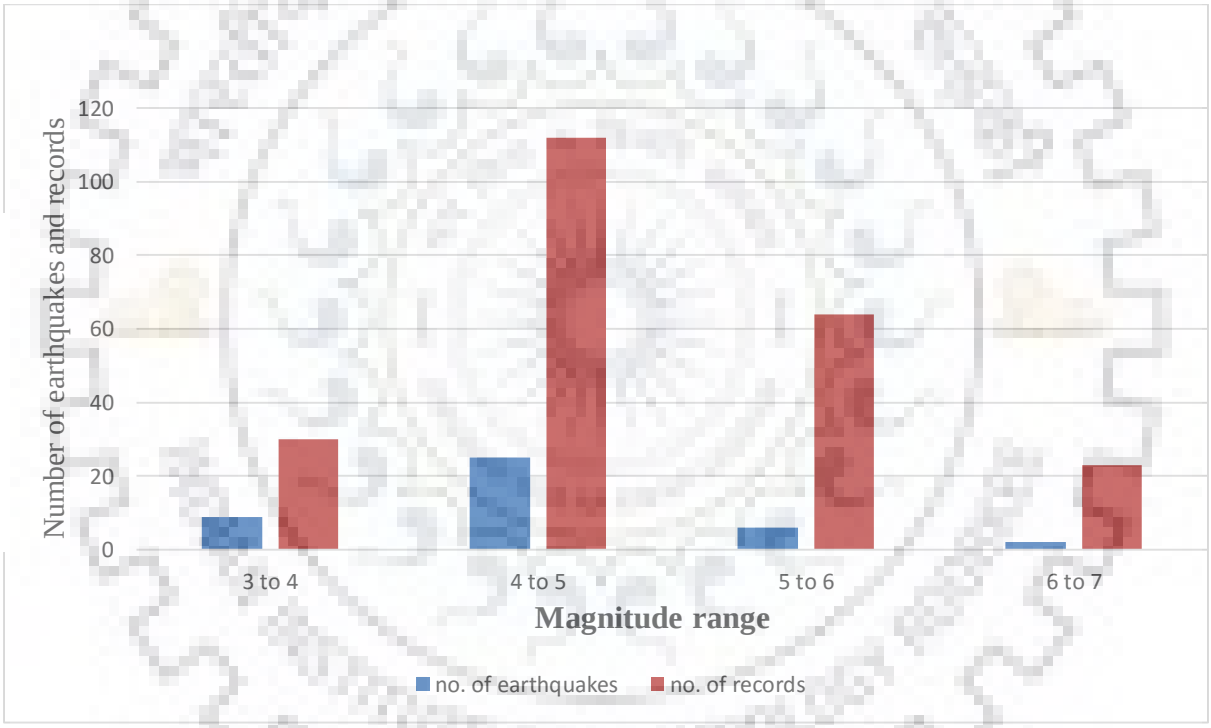


Fig 4.3–graph between magnitude range, no. of earthquakes and no. of records

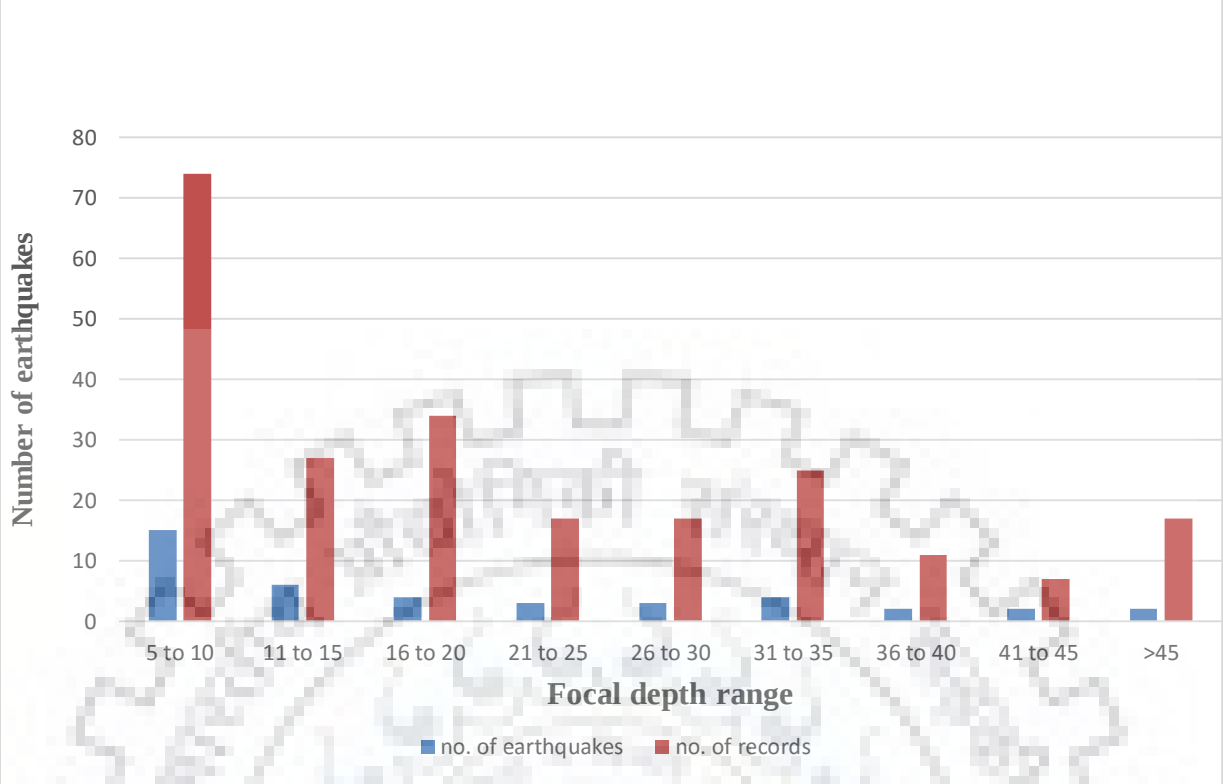


Fig 4.4 - graph between focal depth range, no. of earthquakes and no. of records

## 4.4 DATA CORRECTION

Time histories of a wide range of earthquake magnitudes, epicentral distances and Site Geology parameter, S were taken from PESMOS earthquake database and suitable corrections were applied to make them suitable for usage.

### 4.4.1 BASE LINE CORRECTION

Base Line Correction is of utmost necessity before using a Time history in study and analysis because the effect of uncorrected data would creep up into velocity time history and displacement time history as well and may give unrealistic data [4]. Base line correction is applied by averaging out the data so that all the data oscillates around the y=0 axis.

The digital recordings are often plagued by what we call [3] baseline offsets: small steps or distortions in the reference level of motion [. Although small in acceleration, these offsets can produce completely unrealistic ground displacements (derived from the acceleration traces by double integration). There

may be numerous sources of the offsets (e.g. static buildup in the A/D converter, or tilting of the ground), and for this reason, there is no universal correction scheme that can be applied blindly to the records. Ideally, the physical mechanisms causing the offsets would be known, so that a correction scheme could be tailored for each particular record. In most cases this is too time consuming when dealing with many records from a particular Earthquake, or is impossible because of fundamental uncertainties in the source of the problems. In such cases, the very long period motions must be sacrificed, and a combination of baseline correction and low-cut filtering can be used to produce motions that are accurate representations of the true ground motions at periods of interest to engineers and to many earthquake modelers.[10]

One physical constraint on the ground motion is that the ground velocity be zero, on average, at a sufficiently long time after an earthquake; for this reason, the best way to determine whether there are baseline problems in the recorded acceleration is to look at the velocity obtained by integrating the acceleration. The drift away from zero clearly indicates a baselineproblem, and this problem produces a growing displacement that is clearly unrealistic. The drift in velocity appears to be a straight line.

We adopted the following simple scheme for processing those records; variations of this scheme have been used in processing the records from subsequent earthquakes. The scheme involves fitting a quadratic to the velocity and then filtering, as outlined below

1. Take the acceleration time series a(t). Here we assume that distortion in baseline has a form of quadratic function.
2. Then integrate acceleration time series to velocity time series.
3. Fit a quadratic to velocity, starting at the time of the first arrival and constrained to be 0.0 at the start time.

$$V(t) = a+bt+ct^2 \tag{4.1}$$

Then compute the derivative of fitting function v(t)

$$a`(t) = \frac{dV(t)}{d(t)} \tag{4.2}$$

4. Remove the derivative of the quadratic from the original acceleration time history.

$$a_{corrected} = a(t) - a`(t) \tag{4.3}$$

5. Apply a causal, low-cut ormbsy filter with a subjectively chosen corner frequency.
6. Integrate to velocity and displacement.

Although baseline corrections result in removal of some long-period noise, often low-cut filtering is needed as well. In many cases, filtering is all that is needed, and filtering has the advantage that the effect in the frequency domain is more apparent than when baseline corrections are used. The displacement waveforms and peak displacements are sensitive to the filter corners, the displacement response spectrum is insensitive to the filter corners at periods of engineering interest when the amplitude of the signal at long periods allows the use of relatively low-frequency filter cutoffs.

# CHAPTER 5

## CALCULATIONS AND RESULTS

During an earthquake, the potential energy in the rocks is converted into heat, into mechanical work moving the crustal blocks and crushing the material in the fault zone, and into energy, Es, associated with the emitted elastic waves. At a given period, the energy in the elastic waves is of the form

$$\log_{10} Es = C + 2M, \qquad (5.1)$$

Where C is a constant and M is the earthquake magnitude.

The amount of energy transmitted per unit of time,across unit area, normal to the direction of wave propagation, is $\rho \propto v^2$ for plane P-waves and $\rho\beta v^2$for plane S-waves, where ρis material density, vis velocity of P-waves, β is velocity of S-waves, and v is particle velocity.
The shear-wave energy transmitted through area A during time interval [0, T] is, for example,

$$E_s = \rho A \beta \int_0^t v^2(t)dt \qquad (5.2)$$

with analogous expression for the energy of P-waves. Using Parceval's theorem, it becomes

$$Es = \frac{\rho A \beta}{2\pi} \int_0^\infty \left(\frac{f(\omega)}{\omega}\right)^2 d\omega \qquad (5.3)$$

where F(ω) is the Fourier amplitude spectrum of ground acceleration

## 5.1 SEISMIC WAVE ENERGY:

Earthquake are generated by displacement over a finite length and width of a fault rupture plane as a result of the strain energy build up by tectonic force [14]. Only a very small part of the total energy released during an earthquake is lost in the form of heat and friction over the fault plane and rest is transmitted from the source in all directions in the form of elastic waves. Elastic seismic waves transport the energy both as kinetic energy associated with the motion of the particles of the medium and potential energy associated with the strain developed in the medium[13]. To find this energy, we can model the seismic waves by plane harmonic waves travelling in any direction. The SH-wave with displacement transverse to the direction of the motion can be modeled mathematically by,

$$U(x,t) = A\cos(\omega t - kx);$$

In this expression A is the maximum amplitude of the wave,

$$\omega = 2\pi f = \frac{2\pi}{T} = 2\pi c/\lambda$$

is the frequency of the wave and k is the wave number with λ as the wavelength and c as the wave velocity. The particle velocity at distance x in the direction of motion can be written as,

$$v(x,t) = \frac{\partial u(x,t)}{\partial t} = -A\omega \sin(\omega t - kx)$$

Thus, the kinetic energy of a small volume defined by small area ds of the wavefront and thickness dx is the direction of wave propagation can be defined by,

$$\text{K.E } (E_{kin}) = \frac{1}{2} * \rho * ds * dx * v^2(x,t) = \frac{1}{2} * \rho * A^2\omega^2 \sin^2(\omega t - kx) dx * ds$$

The energy per unit area of wave front per unit distance of wave propagation is given

$$\text{K.E } (E_{kin}) = \frac{1}{2} * \rho A^2\omega^2 \sin^2(\omega t - kx)$$

Also, the shear strain perpendicular to the direction of propagation can be defined by

$$\varepsilon_{ux} = \varepsilon_{xu} = \frac{\partial U(x,t)}{\partial x} = Ak \sin(\omega t - kx)$$

The potential energy stored in the small volume dsdx considered above can thus be defines as the strain energy stored in the volume as

$$PE = \frac{1}{2} * \mu * \varepsilon^2_{ux} = \frac{1}{2} * \mu * \varepsilon^2_{xu} = \frac{1}{2} A^2 k^2 \mu \sin^2(wt-kx) dsdx$$

The energy per unit area of the wavefront per unit distance of wave propagation is given by

$$PE = \frac{1}{2} A^2 k^2 \mu \sin^2(wt-kx) dsdx$$

Since, $k = \omega/c$, we can write

$$\mu k^2 = \mu \frac{\omega^2}{c^2} = \mu \frac{\omega^2}{\mu} \rho = \rho \omega^2$$

Thus,

$$PE = \frac{1}{2} \rho A^2 \omega^2 \sin^2(wt-kx)$$

Summing the KE and PE, the total seismic wave energy per unit area per unit distance along direction of propagation can be defined by,

$$E_s = KE+PE = \rho A^2 \omega^2 \sin^2(wt-kx) = \rho v^2(x,t)$$

From this the energy flux i.e. the energy passes through per unit area of wavefront at distance x per second can be obtained by multiplying with the wave velocity $\beta$ as

$$E_s = \rho \beta v^2(x,t)$$

The total seismic wave energy at distance x for the entire function of the earthquake can be obtained by integrating over the duration of motion

$$E_s = \rho \beta \int_0^T v^2(x,t) dt$$

This expression has been used in the present study to obtain the energy transmitted at a given location using the ground velocity records in the three components of motion as

$$E_s = \rho \beta \int_0^T [v^2{}_x(t) + v^2{}_y(t) + v^2{}_z(t)] dt$$

It can be seen that $2\rho_{source}\beta_{source}A_{source} \sim Es$. The factor of 2 comes from the fact that we approximated the area through which Es is radiated by 2A, representing both sides of the fault plane. It is found that our empirical scaling equations for F(ω), including their extrapolation to the fault surface, are satisfactory and that they can be used for strong-motion estimates of radiated energy.

## 5.2 REGRESSION ANALYSIS

A nonlinear mixed effects model is defined to account for both inter-event and intra-event variability. Most commonly developed attenuation models do not distinguish between these two types of variability [11][12]. The mixed effects model that is proposed describes the covariance structure obtained by careful grouping of the data. Such a model describes the relationship between a response variable, the ground motion parameter, and some covariates in the data that are grouped according to one or more classification (e.g. magnitude). Also, such a model with two sources of random variation is sometimes referred to as a 'hierarchical model' or a multilevel model [9].

To understand the advantages of a mixed effects model, it is useful to consider first a standard fixed effects model, where the form of the attenuation relation may be written as

$$\log Y_k = f(M_k, R_k, S) + \varepsilon_k \quad (5.4)$$

where $Y_k$, $M_k$ and $R_k$ are, respectively, the ground motion parameter (Energy), the magnitude, and the distance for the $k^{th}$ data point (i.e. the observation associated with a single station's ground acceleration record), while S is the site condition and $\varepsilon_k$ is an error term assumed to be normally distributed with mean zero. Importantly, no consideration of the correlation of the data recorded from the same event is included in this fixed effects model.

In direct contrast, in a mixed effects model, the error term in the empirical model development accounts for inter-event and intra-event variability. A mixed effects model is proposed here because such a model accounts from correlation in the data recorded by the same earthquake. The mixed effects model takes the form

$$\log Y_{ij} = f(M_i, R_{ij}, S) + \varepsilon_{ij} + \eta_i \quad (5.5)$$

where $Y_{ij}$ and $R_{ij}$ are the ground motion parameter and distance, respectively, for the $j^{th}$ ground motion recording during the $i^{th}$ event (earthquake). Also, $M_i$ is the magnitude of the $i^{th}$ event; S is the site condition. The error associated with residuals between predicted and observed values of $Y_{ij}$ in this model is comprised of two terms $\varepsilon_{ij}, \eta_i$ . The inter-event term, $\eta_i$ represents between-group variability resulting from differences in the data recorded from different earthquakes, while the intra-event term, $\varepsilon_{ij}$ represents within group variability resulting from differences in the data recorded among the different stations for the same earthquake. These two error terms, $\eta_i$ and $\varepsilon_{ij}$ are assumed to be independent and normally distributed with variances, $\sigma^2$ and $\tau^2$ respectively. The total standard error for this mixed effects model is then $\sqrt{\sigma 2 + \tau 2}$.

## 5.3 REGRESSION MODEL AND RESULTS

In this study the random effect regresion method is used instead of least square fiting method because of consideration of hetrogenity in the data and site. This non linear mixed effect model considers the inter-event variability and intra-event variability [8]. In the attenuation-relationship situation, the mixed effects model can be set to reduce the bias introduced if the data are not distributed evenly among the parameters: for example, if magnitude and distance are statistically correlated, or if the data are dominated by many recordings from few earthquakes or recording sites. One approach of the problem is to seek to enhance the estimation of the coefficients of one earthquake from the data available for others. One such way is to introduce a random-effects model. Brillinger and Preisler (1984, 1985) have proposed a random-effects model to separate the uncertainties associated with between-earthquake (earthquake-to-earthquake) and within-earthquake (record-to-record) variations. Nonlinear mixed-effects models involve both fixed effects and random effects [5]. The regression model used here is as follow:

$$\log_{10}(E) = C1 + C2*M - C3*\log_{10}(\text{distance}) + C4* S$$

Where E is the wave energy which is calculated by using the formula of $\rho\beta v^2$. Where velocity is calculated by integrating the acceleration time history. Then by squaring and integrating the velocity component and multiplying with the density $\rho$ and with $\beta$ we get the energy. C1, C2, C3, C4 are the constants which are calculated by the regression model. These constants are calculated with the fixed effect of C1 + C2 + C3 + C4 ~1.

The values of these constants with the standard errors are as follow:

Table 4.1 – Regression coefficient values and standard error

| | C1 | C2 | C3 | C4 |
|---|---|---|---|---|
| Values | -3.622543 | 1.039407 | 1.363929 | -0.127988 |
| Standard error | 0.4287088 | 0.1042634 | 0.1270322 | 0.0345827 |

So our empirical equation after performing regression and calculating the constant values in the model becomes:-

$$\log_{10}(E) = -3.623 + 1.039*M - 1.364*\log_{10}(\text{distance}) + ( -0.128 )* S$$

As the energy we calculate is per unit area, so to calculate the total energy area is required. This area is calculated as

Area = Fault width * fault length

The fault width = 10^(-1.01+0.32*M) (Km)

Fault length = 10^(-2.44+0.59*M) (km)

To compute the Area for a specifcied Magnitude we used wells coppersmith (1994). we used relation subsurace rupture length specified unspecified fault types.

Table 5.2 – Estimated energy calculations

| M | Fault width | Fault length | Area | Area*const | Energy | Energy_estimated | log(E) =2*M+8.8 |
|---|---|---|---|---|---|---|---|
| 4 | 1.862087137 | 0.831763771 | 1.548817 | 3.12241E+16 | 3.428349 | 1.07047E+17 | 6.30957E+16 |
| 4.5 | 2.691534804 | 1.640589773 | 4.415704 | 8.90206E+16 | 11.34458 | 1.0099E+18 | 6.30957E+17 |
| 5 | 3.89045145 | 3.235936569 | 12.58925 | 2.53799E+17 | 37.5398 | 9.52758E+18 | 6.30957E+18 |
| 5.5 | 5.623413252 | 6.382634862 | 35.89219 | 7.23587E+17 | 124.2211 | 8.98848E+19 | 6.30957E+19 |
| 6 | 8.128305162 | 12.58925412 | 102.3293 | 2.06296E+18 | 411.0541 | 8.47988E+20 | 6.30957E+20 |
| 6.5 | 11.74897555 | 24.83133105 | 291.7427 | 5.88153E+18 | 1360.199 | 8.00006E+21 | 6.30957E+21 |
| 7 | 16.98243652 | 48.97788194 | 831.7638 | 1.67684E+19 | 4500.969 | 7.54739E+22 | 6.30957E+22 |
| 7.5 | 24.54708916 | 96.6050879 | 2371.374 | 4.78069E+19 | 14893.94 | 7.12033E+23 | 6.30957E+23 |
| 8 | 35.48133892 | 190.5460718 | 6760.83 | 1.36298E+20 | 49284.8 | 6.71744E+24 | 6.30957E+24 |

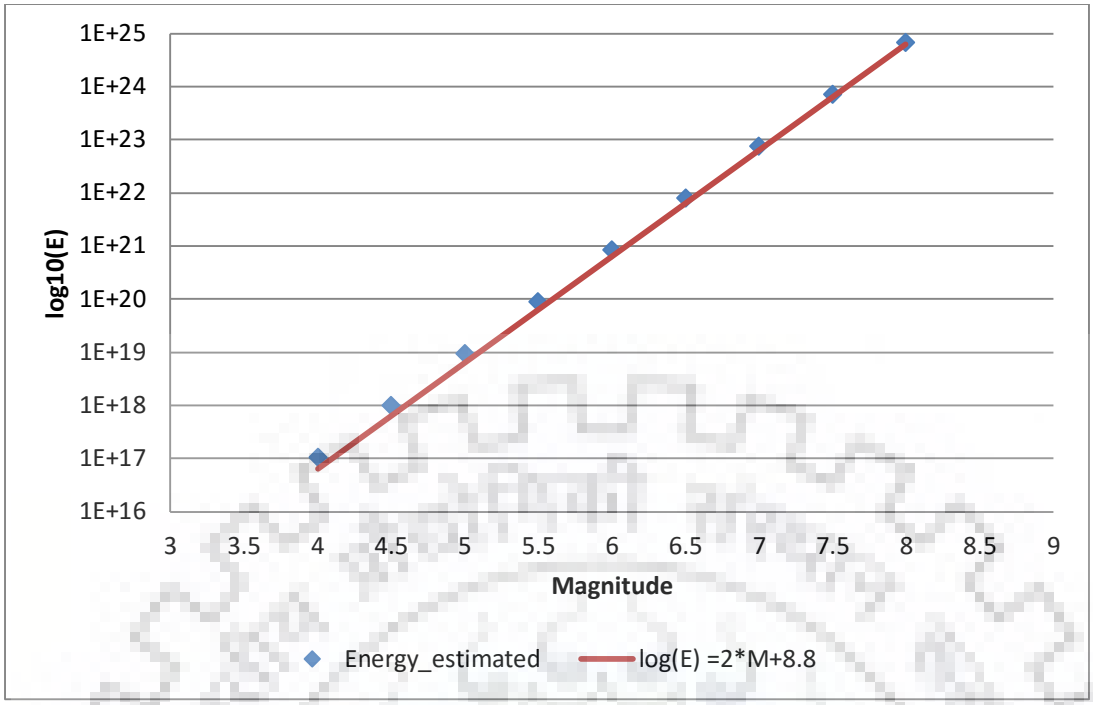


Fig 5.1 – Graph between calculated and estimated energy

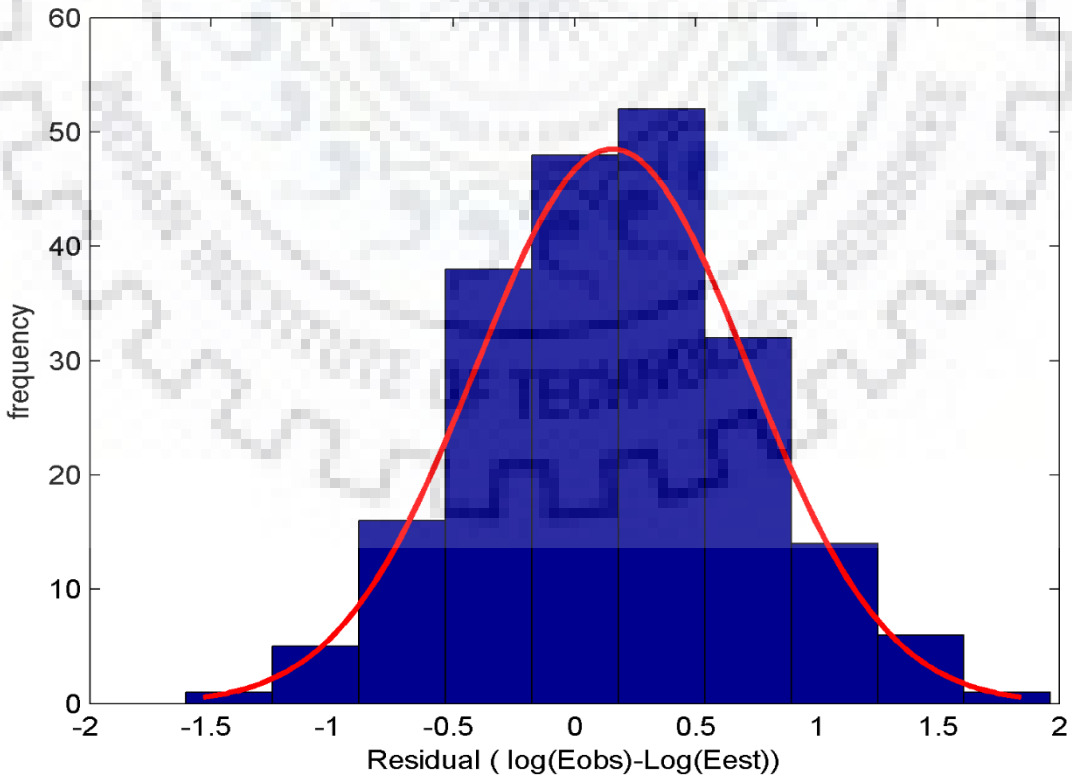


Fig 5.2 – Graph of residual distribution with frequency

# CHAPTER 6

## CONCLUSION

The earthquake energy produced at source point is very high but as it is not the same when distributed in far distance areas, only a fraction of that part reaches to the considered location. So we are considering the energy which reaches the site and will cause damage to the structure. The constants of the regression model are calculated and from the empirical relation formed we can calculate the seismic wave energy at site by knowing only the magnitude and distance energy will be calculated.

The results of regression plotted on graph along with the estimated energy shows that these are approximately equal and shows that our relation formed is correct. The constant values are calculated along with the standard error which limits the value of the constants. As the constant value's range do not include Zero in between them which shows that the result is static and good.

As the seismic energy input, and the seismic energy dissipation during strong shaking can represent the damage potential of an earthquake ground motion more directly than spectral acceleration. Therefore by using these relations we can better estimate the hazard potential of particular earthquake in the region. These can be used for hazard analysis.
This is necessary for the purpose of evolving earthquake resistant design of a new structure or for estimating the safety of an existing structure of importance, like dams, long-span bridges, high-rise buildings, etc. at that site. It is very important for public safety and mitigation of hazards due to destructions of infrastructures such as water, road and highway, and electric power systems, etc

# REFFERENCE


1. Boore, D.M. and Bommer, J.J., 2005. Processing of strong-motion accelerograms: needs, options and consequences. Soil Dynamics and Earthquake Engineering, 25(2), pp.93-115.
2. Boore, D.M., 2005. Long-period ground motions from digital acceleration recordings: a new era in engineering seismology. In Directions in strong motion instrumentation (pp. 41-54). Springer Netherlands.
3. Boore, D.M., 2005. On pads and filters: processing strong-motion data. Bulletin of the Seismological Society of America, 95(2), pp.745-750.
4. Boore, D.M., Stephens, C.D. and Joyner, W.B., 2002. Comments on baseline correction of digital strong-motion data: Examples from the 1999 Hector Mine, California, earthquake. Bulletin of the Seismological Society of America, 92(4), pp.1543-1560.
5. Danciu, L. and Tselentis, G.A., 2007. Engineering ground-motion parameters attenuation relationships for Greece. Bulletin of the Seismological Society of America, 97(1B), pp.162-183.
6. Khashaee, P., Mohraz, B., Sadek, F., Lew, H.S. and Gross, J.L., 2003. Distribution of earthquake input energy in structures. Diane Publishing Company.
7. Kumar, A., Mittal, H., Sachdeva, R. and Kumar, A., 2012. Indian strong motion instrumentation network. Seismological Research Letters, 83(1), pp.59-66.
8. LOH, C.H., 2004, May. Strong motion data processing in Taiwan and its engineering application. In Invited Workshop on Strong-motion Record Processing (pp. 26-27).
9. Massa, M., Pacor, F., Luzi, L., Bindi, D., Milana, G., Sabetta, F., Gorini, A. and Marcucci, S., 2010. The ITalian ACcelerometric Archive (ITACA): processing of strong-motion data. Bulletin of Earthquake Engineering, 8(5), pp.1175-1187.
10. Mollova, G., 2007. Effects of digital filtering in data processing of seismic acceleration records. EURASIP Journal on Advances in Signal Processing, 2007(1), p.029502.
11. Özbey, C., Sari, A., Manuel, L., Erdik, M. and Fahjan, Y., 2004. An empirical attenuation relationship for Northwestern Turkey ground motion using a random effects approach. Soil Dynamics and Earthquake Engineering, 24(2), pp.115-125.

12. Sadigh, K., Chang, C.Y., Egan, J.A., Makdisi, F. and Youngs, R.R., 1997. Attenuation relationships for shallow crustal earthquakes based on California strong motion data. Seismological research letters, 68(1), pp.180-189.
13. Shakal, A.F., Huang, M.J. and Graizer, V.M., 2004, May. CSMIP Strong motion data processing. In Proc. Invitational Workshop on Strong Motion Record Processing.
14. Trifunac, M.D., 2008. Energy of strong motion at earthquake source. Soil Dynamics and Earthquake Engineering, 28(1), pp.1-6.
15. www.pesmos.in, Department of Earthquake Engineering, IIT Roorkee.